The Current Status of Modern Quantitative Fractography

ERVIN E. UNDERWOOD
Georgia Institute of Technology, School of Materials Engineering, Atlanta, GA 30332–0245, USA

ABSTRACT

Modern fractographic research into the old problem of "Quantitative Fractography" has resulted in new theoretical developments based on the powerful relationships of stereology and geometrical probabilities. These efforts have resulted in an assumption-free, statistically-valid procedure for estimating the area of any irregular, rough surface.

Most attempts to model the fracture surface are based on the surface roughness parameter, R_S ($=S_{true}/A_{proj}$) and its relationship to the experimentally available profile roughness parameter, R_L ($=L_{true}/L_{proj}$). Theoretical upper-lower bounds to all R_S, R_L relationships reveal that only one curve, out of a dozen, lies completely within the limits. Moreover, all known data points lie closely around this one parametric roughness curve and within the theoretical limits.

Other procedures for determining R_S include a modified fractal analysis for both profiles and surfaces which yields the "true" values of profile length and surface area. Data obtained by this method are completely compatible with results obtained with the above parametric roughness equation.

Applications of these quantitative procedures to the complex surfaces and profiles of fractured materials have revealed subtle effects not detectable in any other way. These methods also make it possible to perform better failure analyses, develop new fracture resistant materials more expeditiously, and elucidate the effects on the fracture process due to mechanical, chemical and thermal environments.

KEYWORDS

Quantitative fractography; fracture profiles; roughness parameters; modified fractal analysis; stereology; directed measurements; nonplanar surfaces; vertical sections.

INTRODUCTION

The prevention, or actually, the minimization and control of fracture in metals and other structural materials has engaged the attention of scientists and engineers for many years. As material specifications and reliability standards are raised, however, there is a corresponding need for materials with greater fracture-resisting properties. The efficient development of these high-performance alloys requires the ability to quantify the significant attributes of the fracture process.

Recently there has been a revival of interest in the old problem of "quantitative fractography". The principal objective is to describe the features in the fracture surface in terms of their true areas, sizes, spacings, lengths, orientations and distributions. However, the jagged, irregular and reentrant curves and surfaces of metallic materials present seemingly intractable problems. To accomplish this objective, we need to know the area of the fracture surface, which leads to the calculation of the true three-dimensional quantities.

Several factors have played a decisive role in the modern effort to solve these problems. They are:
(1) The application of the fundamental laws of geometrical probabilities and the stereological relationships based on directed measurements.
(2) A generally-valid, linear parametric roughness equation that provides an estimate of the area of a nonplanar surface of any configuration, and
(3) The availability of efficient experimental procedures, using modern image analysis systems with digitizing tablet.

Three experimental approaches have been used extensively in studies of the fracture surface (Underwood,1986). They are based on the SEM fractograph (a projected image)(Broek,1971); stereophotogrammetry (instrumented stereoscopic viewing) (Hilliard,1972); and profilometry (the study of profiles generated by sections through the fracture surface) (El-Soudani,1978). The advantages and disadvantages of each of these methods have been discussed vigorously in the recent literature (Bauer and Haller,1981)(Underwood and Banerji,1987). Although each method has its limitations, the overwhelming experimental choice is profilometry (Underwood,1988).

Profiles are usually generated by means of vertical sections through the fracture surface (Underwood and Chakrabortty,1981). Not only do the profile characteristics relate geometrically to those of the surface, but all minutiae of the crack path are revealed including reentrancies, sub-surface cracking, transgranular and intergranular behavior, etc. The underlying microstructure is also revealed vis-à-vis the crack path (Underwood and Starke,1979). Profiles can also be generated nondestructively by optical means (Tolansky,1952) or by lines superimposed over the fracture surface (Wang, et al.,1982). Once the profile characteristics are known, the true magnitudes of features in three-dimensional sample space can be calculated. It is also possible to calculate the true magnitudes by combining the information from the flat SEM fractograph with the surface (R_S) and profile (R_L) roughness parameters (Underwood,1986a).

In the following discussion, we give some background on stereological relationships, particularly those involving directed measurements, and the various roughness parameters. Then we describe the parametric roughness equations that relate R_S and R_L. Finally, the modified fractal treatment accorded fracture profiles and surfaces is reviewed, and the results are shown to be completely compatible with the parametric analysis.

STEREOLOGICAL BACKGROUND

The quantitative aspects of fractography depend heavily on stereological equations and the interrelationships between random and directed measurements. These topics lead to the subject of roughness parameters and the parametric equations for estimating the fracture surface area.

Stereology is a body of methods for characterizing the spatial geometric properties of microstructures from probabilistic measurements made on planar sections (Underwood,1970) or projections (Underwood,1972). It should be emphasized that "random" structures are not necessary for insuring the validity of stereological relationships. By a "random" configuration we refer to statistically uniform locational and angular distributions of features in a microstructure or fracture surface. If the structure is not random, then random sampling supplies the necessary element of randomness between structure and measurement. In either case, the stereological equations are completely valid.

Random Measurements

The basic equations for volumes, surfaces, lines and number are well-known and have been stated and derived in several treatises. (Underwood,1970)(Weibel,1979)(DeHoff and Rhines,1968) (Saltykov,1974). Here, we will merely note that the spatial quantity sought is usually expressed in terms of the measurements made on planar sections (the metallographic "plane of polish").

If measurements are done manually, the counting measurements are preferred (Underwood,1985)(DeHoff,1986). Only three types of counting measurements are required for most calculations: the point count (P_P); the intersection count (P_L); and the area density count (P_A). These types of measurement procedures are quite efficient and frequently compete favorably in speed and accuracy with semi-automatic image analysis systems.

Adequate statistical coverage usually requires only a few placements of the test grid at various locations and angles in the test plane. The test grid can be marked on a clear plastic sheet: a square array for the P_P-count; a grid of parallel lines for the P_L-count; and a convenient arbitrary test area for the P_A-count.

In principle, random three-dimensional sampling requires section planes at all possible locations and angles through the sample being investigated. However, this extensive statistical coverage is seldom possible or required in practice.

The important stereological equation for length of line in a plane, per unit area, is

$$L_A = (\pi/2)\ P_L \qquad (1)$$

where P_L is the total number of intersections of the grid with the lineal features, divided by the length of the grid lines (within the selected test area). For example, considering a crack trace in the plane of polish, L_A is the ratio of trace length, L_{trace}, to the test area, A_T. This ratio is, of course, equal to the trace length per unit area.

Equations are also available for the area of a fracture surface. The general stereological equation for the area of a surface of any configuration, provided measurements are made randomly, is

$$S_V = 2\ P_L \qquad (2)$$

where S_V is the surface area per unit volume, and P_L is the intersection count with the surface traces, made on one or more random test planes through the surface. Although Eq. (2) is valid for any type of surface (oriented, partially-oriented or random), no information regarding the surface configuration is forthcoming from S_V.

The combination of Eqs. (1) and (2) results in an extremely useful relationship

$$S_V = (4/\pi)\ L_A \qquad (3)$$

which relates the crack surface area per unit test volume to the trace length per unit test area.

Directed Measurements

An important complement to random measurements is called "directed" measurements, or sampling (Saltykov,1974) (Underwood,1970)(Underwood,1987). Sections are cut in preferred directions, and subsequent measurements in these planes may also be taken in preferred directions. These procedures are frequently employed with structures having some degree of preferred orientation in particular directions or planes. This permits the use of special equations appropriate to the special measurements employed. The equations for directed measurements do not supersede the general equations of stereology -- they complement them and provide directional information rather than average values.

If directed measurements are used on a crack trace, several special equations are available. One relationship that involves projected quantities in a preferred direction is

$$(L_A)_{proj} = (P_L)_\perp \qquad (4)$$

where $(L_A)_{proj}$ represents the projected length of the crack along a chosen projection axis, per unit test area, and $(P_L)_\perp$ is the number of intersections with the crack trace, per unit length of a test grid perpendicular to the projection axis. This means that for any single crack trace without reentrancies, the projected

length is a constant equal to the intercepted length on the projection axis. However, if there is significant overlap of the profile, the increased value of $(L_A)_{proj}$ reflects this fact. An overlap parameter based on Eq. (4) will be described later in the Section on "Crack and Microstructural Parameters".

Directed measurements are also used to express the fractional length, L_{or}/L, of an irregular curve of length L that is oriented in a particular direction, L_{or} (Underwood,1970). A parameter that applies to a partially-oriented line in a plane is the degree of orientation, $\Omega_{1,2}$, where the subscripts refer to lines, 1, in a plane, 2. It is defined (Saltykov,1974) by

$$\Omega_{1,2} = \frac{(P_L)_\perp - (P_L)_\parallel}{(P_L)_\perp + 0.571(P_L)_\parallel} \qquad (5)$$

where $(P_L)_\perp$ and $(P_L)_\parallel$ are directed measurements made perpendicular ($\perp$) and parallel ($\parallel$) to the selected orientation axis. $\Omega_{1,2}$ can vary between limits of 0 and 1, where 0 represents no oriented components (a completely random line) and 1 means a completely oriented line (a straight line parallel to the orientation axis). For values in between, the trace can have any degree of partial orientation and $0 < \Omega_{1,2} < 1$.

Directed measurements also give more details about specific surface configurations. Some useful examples are given below. The equation for surfaces projected in a particular direction is

$$(S_V)_{proj} = (P_L)_\perp \qquad (6)$$

where $(S_V)_{proj}$ is the area of the surface projected to a chosen projection plane, divided by the test volume. $(P_L)_\perp$ is an intersection count with the intersection test lines perpendicular to the projection plane.

A parameter for partially-oriented surfaces that invokes directed measurements is the degree of orientation $\Omega_{2,3}$, where the subscripts refer to surfaces, 2, in sample space, 3. Several categories of surfaces have been distinguished (random, planar, linear, and planar-linear) (Saltykov,1974), but here we give only the relationship for partially-oriented planar surfaces

$$\Omega_{p1} = \frac{(P_L)_\perp - (P_L)_\parallel}{(P_L)_\perp + (P_L)_\parallel} \qquad (7)$$

where $(P_L)_\perp$ and $(P_L)_\parallel$ are analogous to the quantities defined in Eq. (5). The values of Ω_{p1} can vary between the limits of 0 and 1 representing, respectively, complete randomness and complete orientation. In between, of course, the surfaces are partially-oriented and $0 < \Omega_{p1} < 1$.

Combinations of the above equations frequently prove useful. For example, equating $(P_L)_\perp$ of Eqs. (4) and (6) gives

$$(S_V)_{proj} = (L_A)_{proj}\ . \qquad (8)$$

We see that, regardless of complexity, the surface projection bears a particularly simple relationship to the profile projection. This equation is also valid for surfaces with or without overlap.

A special case of Eq. (8) is the completely oriented surface represented by a flat plane (Underwood, 1988). It has the minimum area surface when oriented parallel to the projection plane. In this case we see that

$$(S_V)_{or} = (L_A)_{or} \qquad (9)$$

where $(L_A)_{or}$ is measured according to Eq. (4) on section planes perpendicular to the surface. The quantities in Eq. (9) have a fixed value depending, of course, on the dimension of the test volume. For a test cube of edge length a, $(S_V)_{or}$ and $(L_A)_{or}$ equal 1/a.

A related equation pertains to the special case of ruled surfaces (Underwood,1988). These are partially-oriented surfaces that have only one orientation direction, and the surfaces are generated by the translation of a straight line (in any direction) parallel to itself. A ruled surface is shown schematically in Fig. 1. For this case we have

$$(S_V)_{ruled} = (L_A)_{\perp} \qquad (10)$$

where $(L_A)_{\perp}$ refers to a trace on a plane perpendicular to the orientation direction. $(S_V)_{ruled}$ can have any value between 1 and ∞, depending on the complexity of the trace. If the ruled surface is sampled randomly, then Eq.(3) applies.

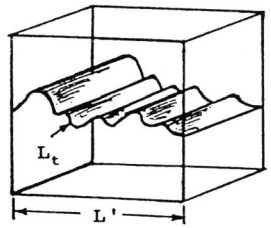

Fig.1. A Ruled Surface.

Note that in (S_V, L_A)-coordinates, Eq. (9) plots as a point, while Eq. (10) plots as a line. Moreover, this line represents the minimum possible values of surface area for all given trace lengths. On the other hand, the maximum values of surface area correspond to those obtained from Eq. (3). The latter equation also plots as a straight line and represents the upper limit for surfaces of any configuration, if sampled randomly. It is important to note that surfaces with random configuration do not require random sampling. For such surfaces, either directed or random measurements should give the same value of S_V.

ROUGHNESS PARAMETERS

Several types of roughness parameters have been proposed for profiles and surfaces (Underwood,1984). A major selection criterion is based on their suitability for characterizing irregular curves and surfaces. It is also desirable that they express roughness well, relate readily to the physical situation, and equate simply to spatial quantities. Because profiles are easily obtained experimentally, it is natural that considerable attention has centered on their properties. Roughness parameters for surfaces are not as numerous (Underwood,1987), possibly because they are too difficult to evaluate experimentally.

Two roughness parameters have been identified that possess outstanding attributes for quantitative fractography. They are the profile roughness parameter R_L (Pickens and Gurland,1976) and the surface roughness parameter R_S (El-Soudani,1978). They are directly related to the basic stereological quantities S_V and L_A, respectively. Other parameters have been proposed, and the more useful of these will also be discussed.

Profile Roughness Parameter

The profile roughness parameter is defined as the true profile length divided by the projected length, or

$$R_L = L_t \; / \; L' \qquad (11)$$

where the prime denotes a projected quantity. The terms in Eq. (11) are depicted schematically in Fig. 2 for a profile in a vertical section plane. An easy, direct way to measure the profile length is to use a digitizing tablet; otherwise, Eq. (1) can be used with manual measurements. Experimental values of R_L between 1.06 and 2.39 have been reported for a variety of materials (Underwood and Banerji,1987). R_L is a dimensionless length ratio that can vary between 1 and ∞. It is independent of configuration and the angular distribution of elements in the profile. As used here, the L' term is projected in a selected direction, thus R_L requires directed sampling for its evaluation.

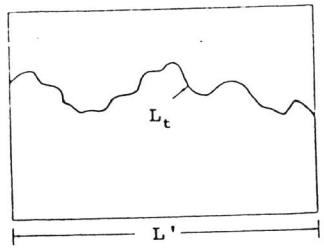

Fig.2. Profile Through a Fracture Surface.

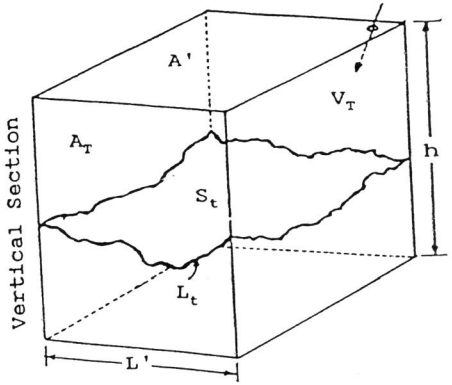

Fig.3. Relationship of Fracture Surface to Other Quantities.

Surface Roughness Parameter

Surface parameters that relate to some particular attribute of the fracture surface may be satisfactory for that restricted purpose (Underwood,1987). However, a parameter that contains the fracture surface area is of more general interest. A natural surface roughness parameter that parallels the profile roughness parameter is R_S, defined as the true surface S_t divided by the projected area A' according to

$$R_S = S_t / A' \quad . \tag{12}$$

Since A' is selected arbitrarily and has a constant value, S_t is obtained directly once R_S is known. R_S is a ratio of areas, thus dimensionless, and can vary between 1 and ∞, depending on the complexity of the surface. Experimental values of R_S are known between 1.1 and 2.4 (Underwood,1988). R_S is independent of configuration and angular distribution of elements in the fracture surface.

Fig. 3 illustrates a test volume V_T containing a fracture surface of area S_t and depicts the geometrical relationships between a trace of length L_t, projection plane A', projection line L', and test area A_T in a vertical section. It is seen that R_S and R_L are closely related. Since the elements of the fracture surface are projected in a designated direction to A', we are concerned here with directed measurements.

Crack and Microstructural Parameters

In addition to the general profile and surface roughness parameters described above, other parameters have been proposed for specific applications. Some parameters are based on the configurational characteristics of the profile; others seek to describe the relationship of the crack characteristics to a particular microstructural feature. Examples of these types of parameters are given below.

The profile configuration parameter, R_P, is essentially the ratio of average peak height, $\overline{H}$, to average peak spacing, $\overline{W}$. As such, it is sensitive to variations in the configuration of an irregular planar curve. The parameter is defined (Behrens,1977) by

$$R_P = (1/2L_T) \int_{y_1}^{y_2} P(y)\, dy \tag{13}$$

where L_T is the (constant) length of the test line; P(y) is the intersection function; and y_1, y_2 are the bounds of the profile envelope in the y-direction. The working expression can be written as

$$R_P = (\Delta y / 2L_T) \sum (P_i)_{\parallel} \quad , \tag{14}$$

where Δy is the (constant) displacement of the horizontal test line of length L_T, and $\sum (P_i)_{\parallel}$ is the total number of intersections of the test line parallel to the orientation axis. Fig. 4 shows the essential elements of this procedure.

The height-to-width ratio comes up frequently in studies of fracture surfaces. The quantity usually measured is $\overline{H}/\overline{W}$, the ratio of the averages, whereas $\overline{H/W}$, the average of the ratios,

is actually desired. Normally, the latter quantity is difficult and time-consuming to obtain. However, in a recent study of dimpled rupture in 4340 steels (Banerji,1986), both $\overline{H}/\overline{W}$ and $\overline{H/W}$ were determined along with R_P. As would be expected, R_P and $\overline{H}/\overline{W}$ values were close (within 13 percent); while $\overline{H/W}$ values, on the other hand, were about three times greater than $\overline{H}/\overline{W}$. Thus, it is important to specify clearly the ratio being used.

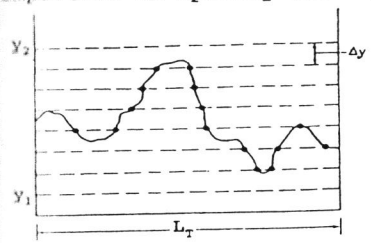

Fig.4. Measurements for Profile Configuration Parameter.

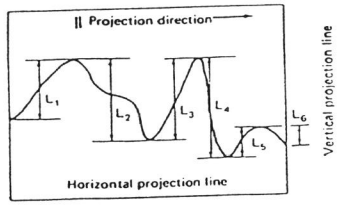

Fig.5. Projection of Profile Segments to Vertical Projection Line.

Another roughness parameter, R_V, is based on the projection of profile lengths in two orthogonal directions (Wright and Karlsson,1983). This parameter is defined by

$$R_V = \sum (L_i')_{\parallel} / \sum (L_i')_{\perp} \tag{15}$$

where the subscripts $\parallel$ and $\perp$ refer respectively to the projection directions parallel and perpendicular to a chosen orientation axis (usually the average crack propagation direction). The projection of length segments in the parallel direction, i.e., $\sum (L_i')_{\parallel}$, is shown schematically in Fig. 5. Note that, in the absence of overlaps or reentrancies, the denominator is a constant equal simply to the projected length of the profile in the perpendicular direction. Alternately, Eq. (15) can be expressed in terms of the intersections with a test grid, according to Eq. (4), by

$$R_V = \sum (P_i)_{\parallel} / \sum (P_i)_{\perp} \tag{16}$$

where here the subscripts $\parallel$ and $\perp$ refer to directions of the grid with respect to the orientation axis. Comparison of Eqs. (14) and (16) reveals that the $\sum (P_i)_{\parallel}$ terms are identical, so in the absence of overlap, R_P and R_V differ only by a constant factor, $\Delta y/2$.

In the case of overlap, a quantitative parameter may be needed to express the extent of such events. A simple expression that accounts quantitatively for overlaps, and avoids the shortcomings of previous offerings, is

$$R_L{}^{OL} = R_L \left[1 + \sum (L_i')_{\perp}^{OL} / (L')_{\perp}^{net} \right] \tag{17}$$

where $\sum (L_i')_{\perp}^{OL}$ is the contribution to the projected length due only to overlaps, and $(L')_{\perp}^{net}$ is the projected length of the profile minus the overlaps. Both quantities are projected perpendicular to the orientation axis, as indicated in Fig. 6. In the absence of overlap, Eq. (17) reduces to Eq. (11).

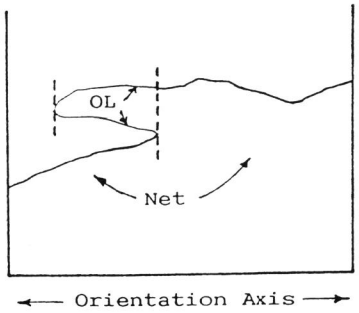

Fig.6. Quantities Involved in the Overlap Correction Model.

The relative projected length due to overlaps can be expressed in terms of intersections with a vertical grid according to

$$\sum(L')_{\perp}^{OL} \;/\; (L')_{\perp}^{net} = \sum(P_i)_{\perp}^{OL} \;/\; \sum(P_i)_{\perp}^{net} \qquad (18)$$

where the number of intersection points in the numerator refer only to the overlapped portions of the profile, and in the denominator to the rest of the curve. The quantity in square brackets in Eq. (17) can also be described as equal to the total projected length over the apparent projected length Underwood,1970).

Gurland has proposed a crack preference index, G, of great generality (Pickens and Gurland,1976). It is defined for the i-th phase by

$$G_i = \sum(L_i)_{ph} \;/\; L_t \qquad (19)$$

where $\sum(L_i)_{ph}$ is the combined lengths of the crack path through the i-th phase, and L_t is the total crack length. Thus, this ratio reveals the fraction of the crack path that passes through a particular phase. In a study of fatigue cracks in aluminum alloys (Underwood and Starke,1979), a modified form of this parameter was used to determine the fraction of transgranular or intergranular cracking. For grains of size 20 μm, $G_{trans} = 0.63$, and for subgrains of size 2 μm, $G_{trans} = 0.39$. The tendency for the crack to prefer a transgranular path through larger grains has been noticed in the past. Other useful crack path-microstructural parameters have been proposed in the literature and discussed in recent reviews (Underwood and Banerji,1987).

PARAMETRIC RELATIONSHIPS

Because of the inherent complexity of fracture surfaces, it is desirable to introduce the assumption-free, general relationships of stereology to help solve the problem of quantifying a fracture surface. This approach is possible because the two major roughness parameters discussed above, R_L and R_S, are directly related to stereological quantities.

Roughness Parameters from Stereological Quantities

The connection of R_S and R_L to their stereological counterparts S_V and L_A can be shown directly starting with Eq. (3),

$$S_V = (4/\pi)\, L_A \;. \qquad (3)$$

Referring to Fig. 3, the surface area per unit volume is

$$S_V = S_t \;/\; V_T = S_t \;/\; A'h \qquad (20)$$

and the trace length per unit area is

$$L_A = L_t \;/\; A_T = L_t \;/\; L'h \;. \qquad (21)$$

Substituting these expressions for S_V and L_A into Eq. (3) yields the equivalent equation in terms of roughness parameters

$$R_S = (4/\pi)\, R_L \;. \qquad (22)$$

Because of the stereological origin of this roughness parameter equation, it is valid for surfaces of any configuration, provided the surfaces are sampled randomly. Usually, however, these roughness parameters are used with directed measurements and different coefficients will apply.

Upper-Lower Bounds to Roughness Parameter Equations

Eq. (22) also applies to random surfaces that are sampled by directed measurements, because a random surface should give the same value (statistically speaking) from any direction. Accordingly, for directed measurements perpendicular to the effective fracture plane, we can write

$$(R_S)_{ran} = (4/\pi)\, (R_L)_{\perp} \;. \qquad (23)$$

This equation represents a straight line when plotted in (R_S, R_L)-coordinate space. It gives the maximum possible value of R_S for any given value of $(R_L)_{\perp}$, up to and including a surface of infinite extent.

The minimum values of R_S, for any given values of $(R_L)_{\perp}$, are obtained from ruled surfaces. In terms of roughness parameters, Eq. (10) becomes

$$(R_S)_{ruled} = (R_L)_{\perp} \qquad (24)$$

where the $\perp$ refers to a sectioning plane perpendicular to the linear elements of the ruled surface. When plotted in (R_S, R_L)-coordinate space, Eq. (24) represents a straight line lying between (1,1) and (∞, ∞) with a slope of 45°.

A special case of Eq. (24) is the perfectly oriented surface with minimum surface area; i.e., a plane. In terms of roughness parameters, Eq. (9) becomes

$$(R_S)_{or} = (R_L)_{or} \;. \qquad (25)$$

Both quantities equal unity when directed measurements are made

perpendicular to the surface. Since the roughness parameters for this plane have a fixed value, the coordinates (1,1) plot as a point and become the origin of the (R_S, R_L)-coordinate axes.

These two limiting curves -- Eqs. (23) and (24) -- enclose an area in (R_S, R_L)-coordinate space. The experimental coordinate points of (R_S, R_L) would be expected to lie only inside this theoretically permissible region. Fig. 7 shows that this is indeed the case for all known roughness data points (Underwood, 1988), including those from a computer simulated fracture surface (Underwood and Banerji,1983).

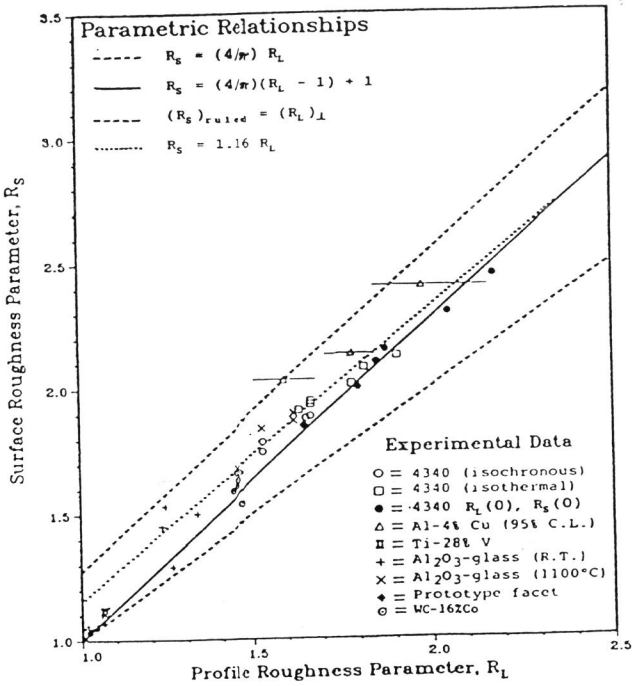

Fig. 7. Upper-Lower Bounds to (R_S, R_L)-Parametric Roughness Equations and Experimental Data Points.

Valid Roughness Parametric Equations

The equations for the upper and lower bounds are obtained readily for the two limiting types of nonplanar surfaces (Underwood,1987). It is a more difficult problem to devise a valid parametric equation for the partially-oriented surfaces between the two bounds. More than ten attempts to express R_S as a function of R_L have been published, but the results show a spread of about 40 percent (Underwood,1988). Different models and assumptions are seen, resulting in different ranges of validity. Some authors have arrived at basically the same (incorrect) equation by using the wrong conditions.

To help identify the valid equations, the general conditions that apply to these parametric expressions are examined. Since R_S and R_L are defined in terms of directed measurements, it is necessary that the parametric equations are also based on directed measurements. The terminal points of the curves must be (1,1) and (∞, ∞). Most importantly, the equation line must lie within the area bounded by the theoretical upper and lower bounds as given by Eqs. (23) and (24).

Five of the ten equations are eliminated because they fail to extend to (∞, ∞). The upper end point for most of these curves was set at $R_S = 2$, $R_L = \pi/2$. This situation probably arose because the difference between S_t/A' $(= R_S)$ and $S_t/\overline{A}'$ $(=2)$ was not recognized. $S_t/\overline{A}'$ is a stereological invariant. If, for example, the surface area is doubled, $S_t/\overline{A}'$ remains constant at 2, but the value of R_S is doubled. Moreover, the specification of a "random" surface as the upper limit, purely on the basis of configuration, is meaningless. It is the magnitude of the surface area that is important, regardless of whether the surface is random or not (Underwood,1987).

The most important criterion is that the lines representing the parametric equations must lie within the theoretically permissible area. The only curve that lies entirely within the bounds and intersects the (1,1)-origin (Underwood,1988) is

$$R_S = (4/\pi)[R_L - 1] + 1 \qquad (26)$$

which represents a "best" line through the permissible region. Eq. (26) appears in Fig. 7 as the heavy central line between the limit curves. The data points fall satisfactorily around the equation line and within the upper-lower bounds.

Because there have been some misunderstandings about the validity of Eq. (26), a brief derivation is given here. We require an equation that represents the gamut of configurations between the completely-oriented plane and the random fracture surface (of infinite extent). Eq. (25) defines the lower point, and Eq. (23) represents the upper point corresponding to the condition of an infinite surface area. The desired equation can be expressed in general form as

$$S_V = K(\Omega)\, L_A \qquad (27)$$

where the limits of the coefficient are $1 \leq K(\Omega) \leq 4/\pi$. $K(\Omega)$ may be considered to be a function of the degree of orientation.

In order to evaluate $K(\Omega)$ over the range of partially-oriented structures between the two extremes set up above, we introduce the intermediate parameter R_f, defined by

$$R_f = (L_t - L')/L_t = 1 - 1/R_L \qquad (28)$$

with L_t and L' as used previously in Eq. (11). The values of R_f vary between 0 (for the oriented case when $L_t = L'$) and 1 (for the extremely complex trace where $L_t \gg L'$); thus, $0 \leq R_f \leq 1$. Assuming linearity between the two extreme configurations, we obtain

$$[K(\Omega) - 1] \,/\, R_f = (4/\pi) - 1 \,. \qquad (29)$$

Combining Eqs. (28) and (29) and substituting into Eq. (27) gives

$$R_S = (4/\pi)[R_L - 1] + 1 \quad , \tag{26}$$

the only parametric roughness equation that complies with all the general conditions given above.

A two-parameter roughness equation has also been proposed (Underwood,1986a). It involves explicitly both R_L and $\Omega_{1,2}$ (as defined by Eq. 5) and has the form

$$R_S = \{(4/\pi) - [(4/\pi) - 1]\Omega_{1,2}\}R_L \quad . \tag{30}$$

This equation has the capability of covering the entire permissible area merely by fixing the various values of $\Omega_{1,2}$ between 0 and 1. Since R_L is a magnitude-dependent quantity and $\Omega_{1,2}$ reflects the configurational aspects of the profile, Eq. (30) provides more information about the fracture surface than the single line embodied in Eq. (26).

A simplified but effective relationship between R_S and R_L has been proposed recently (Gokhale and Underwood,1988). For the case of no overlap, the equation is

$$R_S = 1.16\ R_L \quad . \tag{31}$$

It is an extension of the Scriven and Williams analysis of the angular variation of profile and surface elements (Scriven and Williams,1965). R_S is expressed in terms of a series in R_L, with Eq.(31) representing only the first term of the series. Thus the lower point of (1,1) in R_S, R_L is not attained. However, excellent agreement is obtained with experimental data points within the range of R_L = 1.2 to 2.0 .

Eqs. (26) or (31) provide estimates of R_S. Once R_S and R_L are available, corrections can be made to measurements from the flat SEM fractograph. Examples of applications to actual fracture features have been given. (Underwood,1986a) (Underwood,1986b) (Underwood and Banerji,1987).

Because the values obtained for data points and from equations depend on the accuracy with which R_L has been obtained, it is important to assess the possible errors that could arise. One question to be answered is the effect of fractal variations on the measured profile lengths. This is discussed in the next section.

FRACTALS APPLIED TO FRACTOGRAPHY

As shown in Fig. 7, all known experimental values of (R_S, R_L) lie within the two limiting curves. However, their exact locations are dependent on the accuracy with which L_t, and thus R_L, has been determined. The same considerations apply to R_S, since it bears a direct relationship to R_L. Because some fracture profiles are extremely irregular, they have been investigated for their fractal characteristics. Surprisingly enough, natural irregular curves do not appear to possess self-similitude in the sense of Mandelbrot (Mandelbrot,1982). The results of current developments in this area are presented below.

Current Investigations

Although there has been a tremendous surge of research on various aspects of fractals in materials, fractal studies of fracture are relatively scarce. Recent reviews (Underwood and Banerji,1986) (Underwood and Banerji,1987) have described the general state of knowledge in this area, while a few research papers have dealt specifically with fractals in metals (Wright and Karlsson,1983) (Chermant, et al.,1987)(Pande, et al.,1987)(Banerji,1988) (Wasén and Karlsson,1988), ceramics (Mecholsky, et al.,1986) (Mecholsky, Passoja and Feinberg,1988), composites(Davidson,1987) (Feinberg-Ringel,1988)(Drury,1988) and rubber (Stupak and Donovan,1988). The relationship of fractal properties to fracture toughness (Mandelbrot, Passoja and Paullay,1984) (Richards and Dempsey,1988), fracture mechanics (Williford,1988)(Rosenfield, 1987) and fatigue (Ivanova,et al.,1989)(Banerji,1986) have also been considered.

The central parameter in the fractal treatment of irregular planar curves is the fractal dimension, D, which appears in the exponent of the original Richardson-Mandelbrot equation (Mandelbrot,1982)

$$L(\eta) = L_o\, \eta^{-(D - 1)} \tag{32}$$

where the apparent profile length, $L(\eta)$, is expressed in terms of the size of the measuring unit, η . The value of D is obtained from the linear form of the equation

$$\log L(\eta) = \log L_o - (D - 1)\log \eta \quad . \tag{33}$$

A plot of $\log L(\eta)$ vs $\log \eta$ is called the fractal plot. A straight line (which approaches ∞ as η approaches 0) is predicted, yielding a constant value of D.

Instead of a straight line, however, an extensive experimental study (Banerji and Underwood,1984) revealed fractal curves with a reversed sigmoidal shape. An example is given in Fig. 8. These reversed sigmoidal curves (RSC) show a pronounced asymptotic trend, tending toward a fixed value of $L(\eta)$ as η approaches 0. Thus the fractal dimension D does not have a constant value. An asymptotic limit is understandable, of course, because of the ultimate limitation represented by the size of the atom. Deviations from linearity were not detected in early work, primarily because the range in η-sizes (by a factor of only 10 to 20 times) was too small to establish the complete fractal curve (Underwood and Banerji,1987). In later work, researchers noticed a tendency toward deviation from a straight line in their fractal plots, giving rise to such terms as "semi-fractal" (Rigaut, et al.,1985) or "critical resolution point" (Paumgartner, et al.,1981).

Modified Fractal Analysis

In an effort to rectify this situation, a linearization procedure was proposed (Underwood and Banerji,1986) that not only gives a constant modified fractal dimension, but also a "true" value of the profile length, L(0), which corresponds to $L(\eta)$ as η approaches 0.

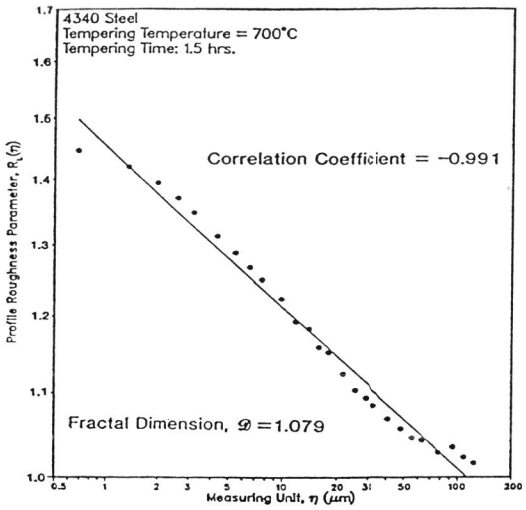

Fig.8. Data Points Revealing a RSC Fractal Plot.

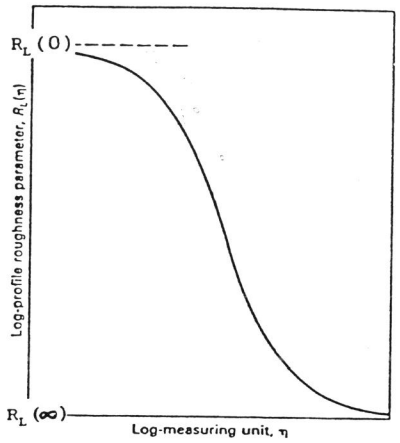

Fig.9. RSC Model Showing Upper and Lower Asymptotic Limits to $R_L(\eta)$.

Extensive fractal data were obtained over a range in η of about 650 times -- about 25 times greater than any range previously reported. Thus the full fractal plot is obtained and clearly reveals the asymptotic behavior at small η. A significant improvement was effected by dividing the profile projected length (a constant) into Eq. (32), giving

$$R_L(\eta) = C\,\eta^{-(D-1)}. \tag{34}$$

The profile roughness parameter now provides a lower asymptotic limit which approaches 1 as η approaches ∞.

The presence of two asymptotic limits to the RSC permits a linearization procedure based on a standard treatment of sigmoidal curves as commonly encountered in phase transformation studies. Fig. 9 shows the RSC model adopted with asymptotic limits of $R_L(0)$ as $\eta \to 0$, and $R_L(\infty) \to 1$ as $\eta \to \infty$.

Linearized RSC Fractal Curves. The general expression for fraction transformed in the forward reaction has a sigmoidal shape (Underwood and Banerji,1987). It is given by

$$y_F = 1 - e^{-\alpha t^{\beta}} \tag{35}$$

where α and β are constants and t is the reaction time. For the reverse reaction (a RSC), we note simply that $y_R = 1 - y_F$, which gives

$$y_R = e^{-\alpha t^{\beta}}. \tag{36}$$

To linearize this expression, double logs of both sides are taken, resulting in

$$\log\log(1/y_R) = \log(\alpha/2.3) + \beta \log t. \tag{37}$$

Replacing t by η and expressing y_R in fractional form yields

$$y_R = \frac{R_L(\eta) - R_L(\infty)}{R_L(0) - R_L(\infty)} = \frac{R_L(\eta) - 1}{R_L(0) - 1}. \tag{38}$$

Substitution gives the linear equation for profiles according to the modified fractal analysis

$$\log\log\frac{R_L(0) - 1}{R_L(\eta) - 1} = C_1 + \beta \log \eta. \tag{39}$$

C_1 is a constant and β is the slope, analogous to the slope expressed in Eq. (33). The curve will be linear if $R_L(0)$ has the correct value. The best value can be determined by iterative optimization (Banerji,1988), or graphically, until the plot of Eq.(39) is best linearized. It should be noted that $R_L(0)$ represents the "true" length of the profile, i.e., as η approaches 0.

In addition to this treatment for RSC profiles, a fractal equation for irregular surfaces, comparable to that for profiles, has also been proposed (Underwood and Banerji,1986). Its major characteristic is that it is based on an area measurement unit η^2 rather than a length unit. The development of this new fractal equation for surfaces leads to a linear form analogous to Eq.(39) for profiles, such that

$$\log\log\frac{R_S(0) - 1}{R_S(\eta^2) - 1} = C_2 + \gamma \log \eta^2 = C_2 + 2\gamma \log \eta. \tag{40}$$

Here, the LHS may be plotted against either $\log \eta^2$ (with slope equal to γ) or, for convenience, against $\log \eta$ (with slope equal to 2γ). The value of $R_S(0)$ is estimated by an iterative optimization procedure similar to that used to determine $R_L(0)$. Furthermore, the surface area obtained from $R_S(0)$ represents the "true" area of the surface, independent of fractal variations in η^2.

Plots of experimental fractal data in Fig. 10 show that Eqs.(39) and (40) are linear over a wide range of η (Underwood and Banerji,1986). Thus, the β and γ slopes are satisfactory measures of the fractal characteristics of natural RSC profiles and surfaces.

Modified Fractal Dimensions. If desired, β can be related to the conventional Mandelbrot fractal dimension, D, for profiles. To accomplish this, a modified fractal equation for RSC profiles is needed. This can be expressed as

$$R_L(\eta) = C_3\,\eta^{-(D_L - 1)} \tag{41}$$

where D_L is the RSC fractal dimension for (linear) profiles.

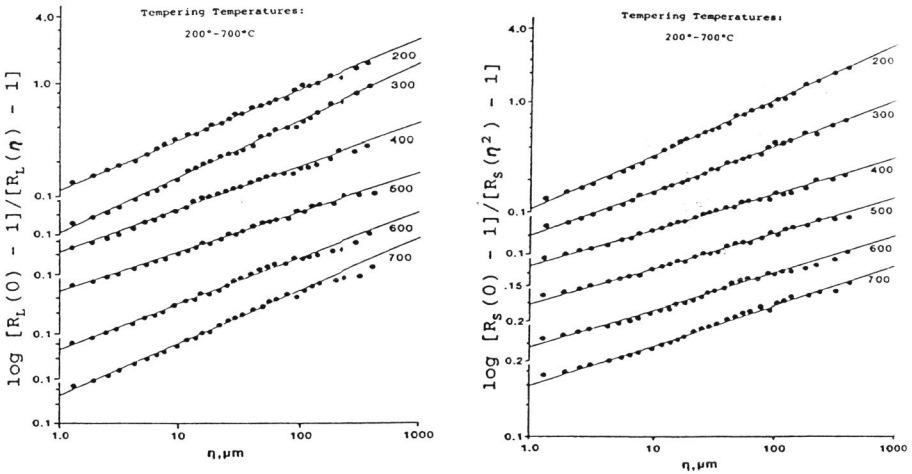

Fig.10. Linearized RSC Fractal Data for 4340 Specimens.
(a) Profiles. (b) Surfaces.

A new fractal equation, comparable to that for profiles, was also developed for irregular RSC surfaces (Underwood and Banerji,1986). It has the form

$$R_S(\eta^2) = C_4 \ [\eta^2]^{-(D_S - 2)/2} \qquad (42)$$

where D_S is the corresponding RSC fractal dimension for surfaces. C_3 and C_4 are constants. To evaluate D_L and D_S, the (absolute) values of the slopes of Eqs. (41) and (42) are equated to β and γ in Eqs.(39) and (40), respectively, resulting in

$$D_L = \beta + 1 \qquad (43)$$

and

$$D_S = 2\gamma + 2. \qquad (44)$$

Typical values for a series of 4340 fractured steels give $(D_S - D_L) \approx 1$, which is very satisfactory from a fractal point of view. Moreover, $D_L > 1$ and $D_S > 2$, as required by fractal theory.

Fractal Roughness Parameters

The above treatment of upper-lower bounds defines the theoretically permissible region in (R_S, R_L)-coordinate space where roughness parameter points must lie. It was also noted that the locations of the experimental (R_S, R_L)-coordinate points depend, among other things, on the fractal variability of L_t with η-size.

The RSC analysis described above circumvents this fractal indeterminancy by means of the "true" values of profile length and surface area as expressed by $R_L(0)$ and $R_S(0)$. A test of the physical validity of these constants is afforded by the (R_S, R_L) plot in Fig. 7 (Underwood,1988). The open circles represent six experimental values of (R_S, R_L) measured at $\eta = 0.683$ μm.

When recalculated in terms of the "true" values, $R_L(0)$ and $R_S(0)$, these same six points appear as filled circles at higher values, as would be expected. This confirmation of the parametric roughness equation, Eq. (26), is noteworthy, and helps enhance the credibility of the modified fractal analysis.

SUMMARY

A general treatment of fracture surface geometry has been developed based on the powerful relationships of stereology and geometrical probabilities. These efforts have resulted in an assumption-free, statistically-valid procedure for the quantitative estimation of the magnitude of features in an irregular, rough, non-analytic surface.

Most attempts to model the fracture surface are based on the Surface Roughness Parameter, R_S, and the linear Profile Roughness Parameter, R_L. R_S contains the fracture surface area and is relatively inaccessible, while R_L is experimentally available from profiles generated by vertical sections through the fracture surface.

Theoretical upper-lower bounds to all R_S, R_L relationships reveal that only one equation, out of a dozen, lies completely within the limits. This Parametric Roughness Equation is

$$R_S = (4/\pi)\ [R_L - 1] + 1 \ .$$

All known data points -- for metals, ceramics, composites, and a computer simulated fracture surface -- lie within the bounds, and cluster closely around the above parametric roughness equation line.

The roughness parameters R_S and R_L enable corrections to be made to conventional measurements on the flat SEM fractograph (a projected image) giving the best estimates of the actual spatial quantities. Corrections of over 100 percent have been reported.

Because of the fractal indeterminancy in the measured profile length L_t (and thus R_L), a modified fractal analysis has been developed, including a new fractal equation for irregular surfaces. Moreover, "true" values of the roughness parameters, $R_S(0)$ and $R_L(0)$, are obtained from the modified analysis. These scale independent parameters provide the best estimates of the actual profile length and fracture surface area, and conform well to the above parametric roughness equation.

ACKNOWLEDGMENT

This appraisal was made possible through the support of the National Science Foundation, Division of Materials Research, Metallurgy Program, under Grant No. DMR-8504167.

REFERENCES

Banerji, K. (1986). Quantitative Analysis of Fracture Surfaces Using Computer Aided Fractography, Ph.D. Thesis, Georgia Inst. of Technology.

Banerji, K.(1987). In M. Kališnik, Ed., Proc. 7th Int. Congr. for Stereology, Caen,France. Publ. in Ljubljana, Yugoslavia,815-820

Banerji, K.(1988). Quantitative Fractography: A Modern Perspective, Metall. Trans. 19A No. 4, 961-971.

Banerji, K. and E.E.Underwood (1984). In S.R.Valluri, et al. Eds.,Advances in Fracture Research, Vol.2, Proc. 6th Int. Conf. on Fracture, New Delhi, India,1371-1378.

Bauer, B. and A. Haller (1981).Pract. Metallography 18 327-341.

Behrens,E.W.(1977). Personal communication.

Bryant, D.(1987). Micron & Microsc. Acta 17 No.3, 237-242.

Chermant,L., J.-L.Chermant and M. Coster(1987). In M.Kališnik, Ed., Proc.7th Int. Congr.for Stereology, Caen,France. Publ. in Ljubljana, Yugoslavia, 845-850.

Davidson,D.L.(1987). Interim Tech. Rep. to ONR, Southwest Res. Inst.

DeHoff,R.T.(1986).Chap.7. In G.F.Vander Voort,Ed., Applied Metallography, Van Nostrand Reinhold, 89-99.

DeHoff, R.T. and F.N.Rhines (1968). Quantitative Microscopy, McGraw-Hill, New York.

Drury, W.J.(1988).Quantitative Microstructural and Fractographic Characterization of an Al-Li/FP Metal Matrix Composite, MS Thesis, Georgia Inst. of Techn.

El-Soudani,S.M. (1978). Profilometric Analysis of Fractures, in Metallography 11, 247-336.

Feinberg-Ringel,K.S.(1988). Quantitative Fractographic Analysis of Al_2O_3/Al-2.5%Li Metal Matrix Composite, MS Thesis, Georgia Inst. of Techn.

Gokhale,A.M. and E.E.Underwood(1988). A New Parametric Roughness Equation for Quantitative Fractography, submitted to Acta Stereologica, Ljubljana, Yugoslavia.

Hilliard, J.E.(1972). J. Microscopy, 95 Pt.1, 45-58.

Ivanova,V.S., S.A.Kunavin, and A.A.Shanjavshij(1989). Quantitative Fractography, Self-Similarity and Fractal Nature of Metal Fatigue Fracture, submitted to Proc.7th Int. Conf. on Fracture, Houston, TX.

Mandelbrot,B.B.(1982). The Fractal Geometry of Nature, H.Freeman,CA.

Mandelbrot,B.B., D.E.Passoja and A.J.Paullay(1984), Nature (London) 308 [5961], 721-722.

Mecholsky,J.J., et al.(1986). Fractal Aspects of Materials, Mat. Res.Soc. 5 .

Mecholsky, J.J., D.E.Passoja, and K.S.Feinberg(1988). Qualitative Analysis of Brittle Fracture Surfaces Using Fractal Geometry, J. Amer.Cer.Soc. To be published.

Pande, C.S., L.E.Richards, N.Louat, B.D.Dempsey and A.J.Schwoeble (1987). Acta Metall. 35 1633-1637.

Paumgartner, D., G. Losa and E.R.Weibel(1981). J. Microscopy, 121 Pt.1, 51-63.

Pickens, J.R. and J. Gurland (1976). In E.E.Underwood, R. de Wit and G.A.Moore,Eds. Proc.4th Int. Congress for Stereology,NBS 431, National Bureau of Standards, 269-272.

Richards, L.E. and B.D.Dempsey(1988). Scripta Met. 22 687-689.

Rigaut,J.P., P.Berggren and B.Robertson(1987). Stereology, Fractals and Semi-fractals, Acta Stereologica 6 63-67.

Rosenfield,A.R.(1987). Fractal Mechanics, Scripta Met.21 1359-1361.

Saltykov,S.A.(1974). Stereometrische Metallographie, VEB Deutscher Verlag für Grundstoffindustrie, Leipzig,DDR.

Scriven, R.A. and H.D.Williams(1965). Trans. AIME 223 1593-1602.

Shieh,W.T.(1974). Metall. Trans. 5,1069-1085.

Stupak, P.R. and J.A.Donovan(1988). Fractal Analysis of Rubber Wear Surfaces and Debris, J.Materials Sci., to be published.

Underwood,E.E.(1970). Quantitative Stereology Addison-Wesley,MA.

Underwood, E.E.(1984). In J.L.McCall and J.H.Steele,Eds. Practical Applications of Quantitative Metallography, ASTM, STP 839, 160-179.

Underwood,E.E.(1985). Quantitative Metallography, in ASM Metals Handbook, 9th Ed., Metallography and Microstructures, Vol.9, Metals Park, OH,123-134.

Underwood,E.E.(1986). Analysis of Fracture Roughness Parameters, presented at 1st Int. Conf. on Microstructology, Univ. of Florida, Gainesville, FL.

Underwood,E.E.(1986a). Quantitative Fractography, Chap. 8. In G.F. Vander Voort, Ed. Applied Metallography, Van Nostrand Reinhold, 101-122.

Underwood,E.E.(1986b). J. Metals 38 No.4, 30-32.

Underwood,E.E.(1987). Stereological Analysis of Fracture Roughness Parameters. In M.Kališnik,Ed., Commemorative Memorial Volume of Acta Stereologica,Twenty-five Years of Sterology, Ljubljana, Yugoslavia, 169-178.

Underwood,E.E.(1988). ASM Materials Science Seminar, Cincinnati, OH.To be published.

Underwood,E.E. and K.Banerji(1983). Statistical Analysis of Facet Characteristics in a Computer Simulated Fracture Surface, In M.Kališnik, Ed., Proc. 6th Int. Congr. for Stereology, Gainesville, Fla., Ljubljana, Yugoslavia, 75-80.

Underwood,E.E. and K. Banerji(1986). Fractals in Fractography, Mater.Sci.& Eng.80, 1-14.

Underwood, E.E. and K. Banerji (1987). Quantitative Fractography, in ASM Metals Handbook, 9th Ed. Fractography and Atlas of Fractographs, Vol. 12, Metals Park, OH, 193-210.

Underwood,E.E. and K.Banerji(1987a). Fractal Analysis of Fracture Surfaces, ibid.211-215.

Underwood,E.E. and S.B.Chakrabortty(1981). In L.N.Gilbertson and R.D.Zipp, Eds. Fractography and Materials Science,ASTM, STP 733, 337-354.

Underwood, E.E. and E.A.Starke (1979).In J.T.Fong,Ed.,Fatigue Mechanisms, ASTM, STP 675, 633-682.

Wang,R., B.Bauer and H.Mughrabi (1982). Z. Metallkunde 73 30-34.

Wasén,J. and B.Karlsson(1988). The Geometrical Interpretation of Fractals in Quantitative Fractography, Proc. 8th Int. Conf. Strength of Metals and Alloys, Pergamon Press, in print.

Weibel, E.R. (1979). Stereological Methods, Vols. 1 and 2, Academic Press, London.

Williford,R.E.(1988). Scripta Met. 22 197-200.

Wright,K. and Karlsson,B.(1983). J.Microscopy, 129 Pt.2, 185-200.